Supporting Information –

Learning from Nature: Molecular Rearrangement in Bismaleimide System Leading to Dramatic Increase in Impact Strength

Mohammad Hamza Kirmani, Prabhakar Gulgunje, Jyotsna Ramachandran, Pedro J. Arias-Monje, Po-Hsiang Wang, and Satish Kumar,*

School of Materials Science and Engineering, Georgia Institute of Technology, Atlanta, GA, 30332, USA

E-mail: satish.kumar@mse.gatech.edu

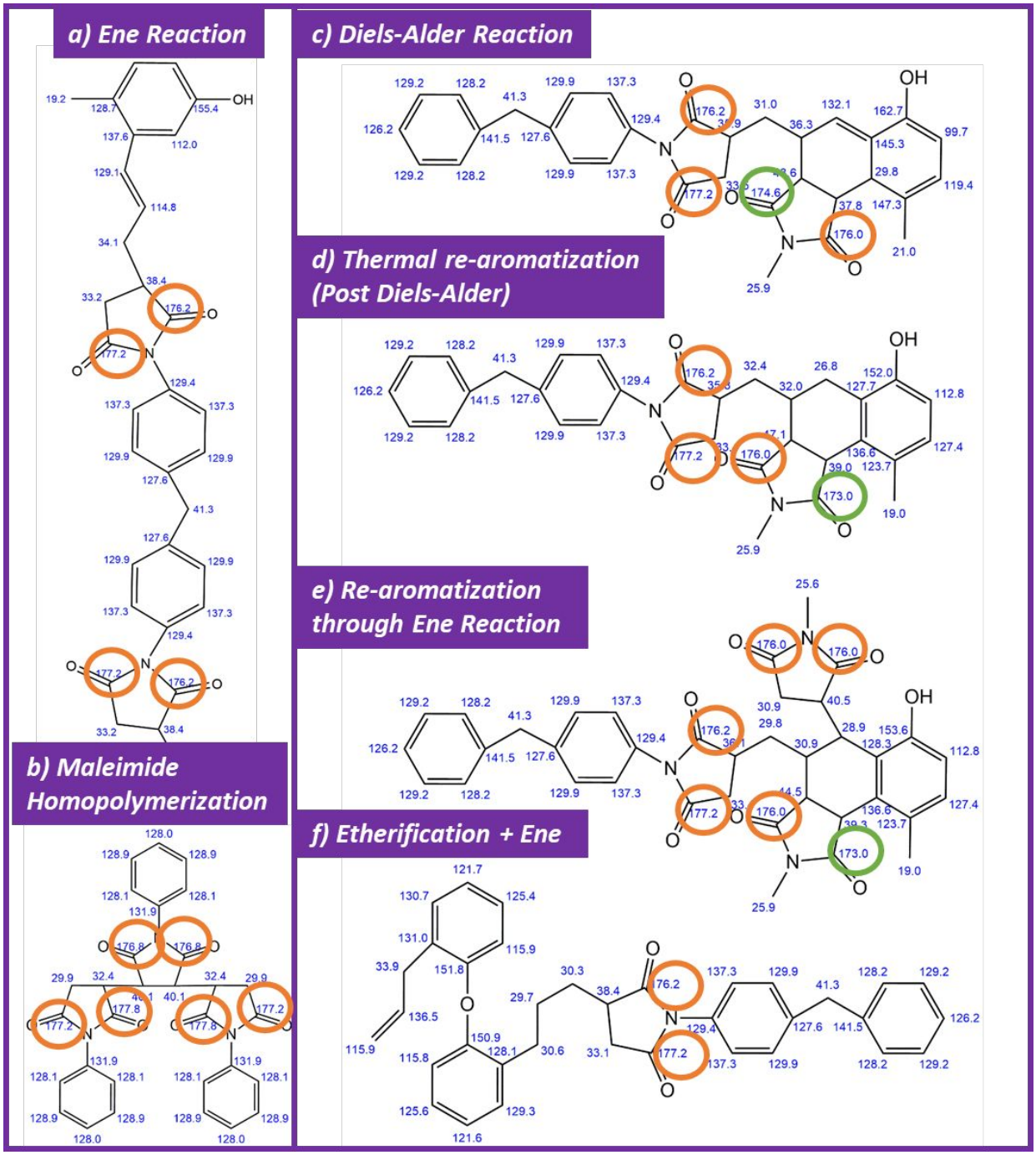

Figure S1 : Predictions of ^{13}C NMR shift for the various possible structures expected to be formed upon curing[1–5] of BMI, using ChemDraw Professional software. The orange circles highlight the carbonyl groups contributing to ^{13}C NMR shifts between 177.8-176 ppm whereas the green circles highlight the carbonyl groups contributing to ^{13}C NMR shifts between 174.6-173 ppm.

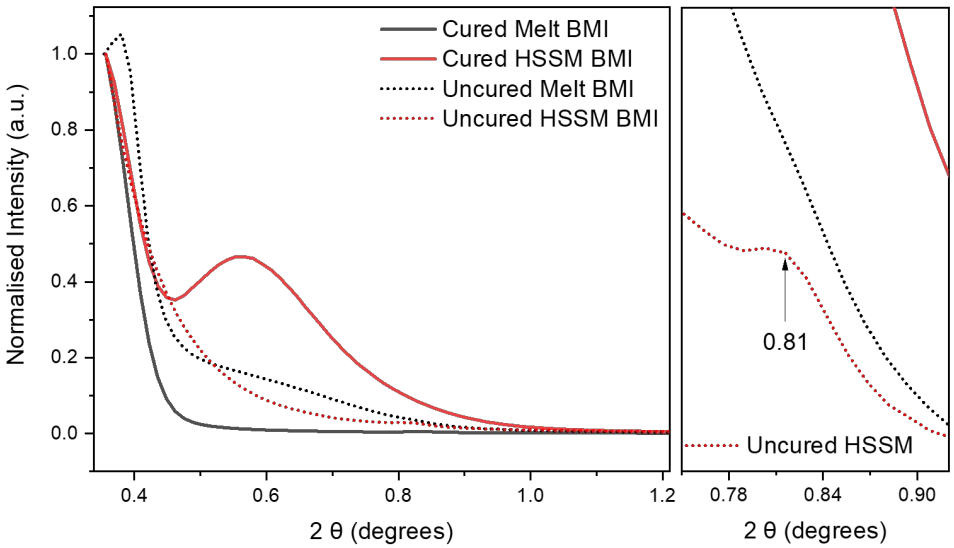

Figure S2 : SAXS plots of both uncured and cured BMI processed through Melt and HSSM. While uncured Melt BMI demonstrated a peak at 0.38 2θ suggesting heterogeneity, potentially from clustering of individual components, the uncured HSSM demonstrates a rather homogenous system with a minor peak at 0.81 2θ.

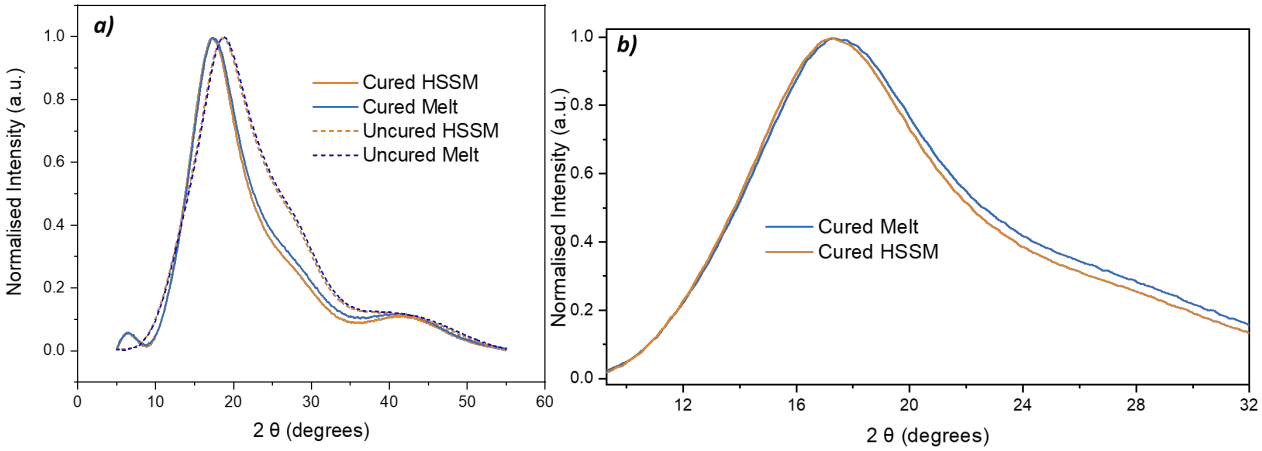

Figure S3 : (a and b) WAXD of cured and uncured Melt and HSSM BMI. (a) Differences between the uncured and cured specimens could be observed. No significant differences between cured Melt and cured HSSM or uncured Melt and uncured HSSM are observed. (b) Magnified diffractogram of the cured Melt and HSSM BMI.

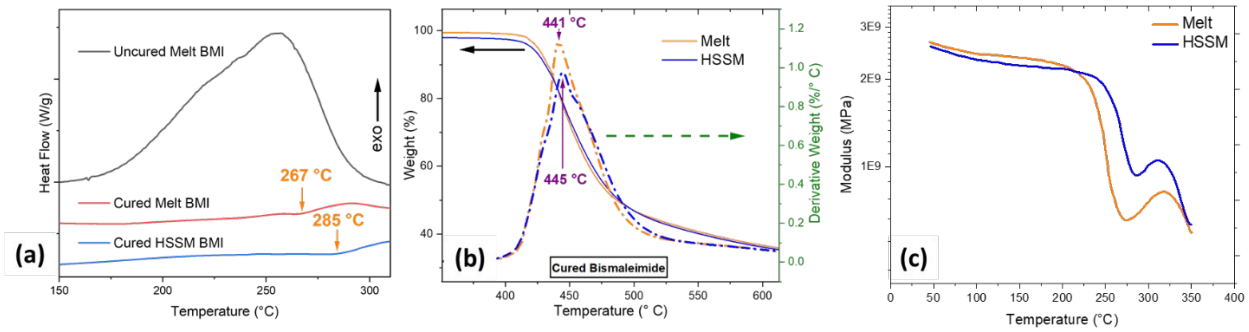

Figure S4 : (a) DSC plots of uncured melt BMI, cured Melt and HSSM BMI at 10 °C/min heating rate in air atmosphere. The plots have been shifted along the y axis for ease of comparison. Cured Melt and HSSM BMI exhibit no exothermic peak related to heat of cure as could be seen for the uncured melt BMI, thus suggesting that both samples undergo complete curing. A change in the heat capacity is observed in cured melt BMI starting at about 267 °C and in cured HSSM melt BMI starting at about 285 °C. These temperatures are in close agreement with T_g values observed through DMA. (b) Thermal degradation of cured Melt and HSSM is determined using TGA under N_2 atmosphere at 10 °C/min heating rate. The peak position of the derivative curve of weight with temperature is taken as the degradation temperature. (c) Storage modulus of cured HSSM and Melt BMI with temperature. The discrepancy in the storage modulus at room temperature obtained through DMA and the Young's modulus obtained through universal tensile machine (Table S7) could result from the difference in the test conditions and instrument compliance.[6]

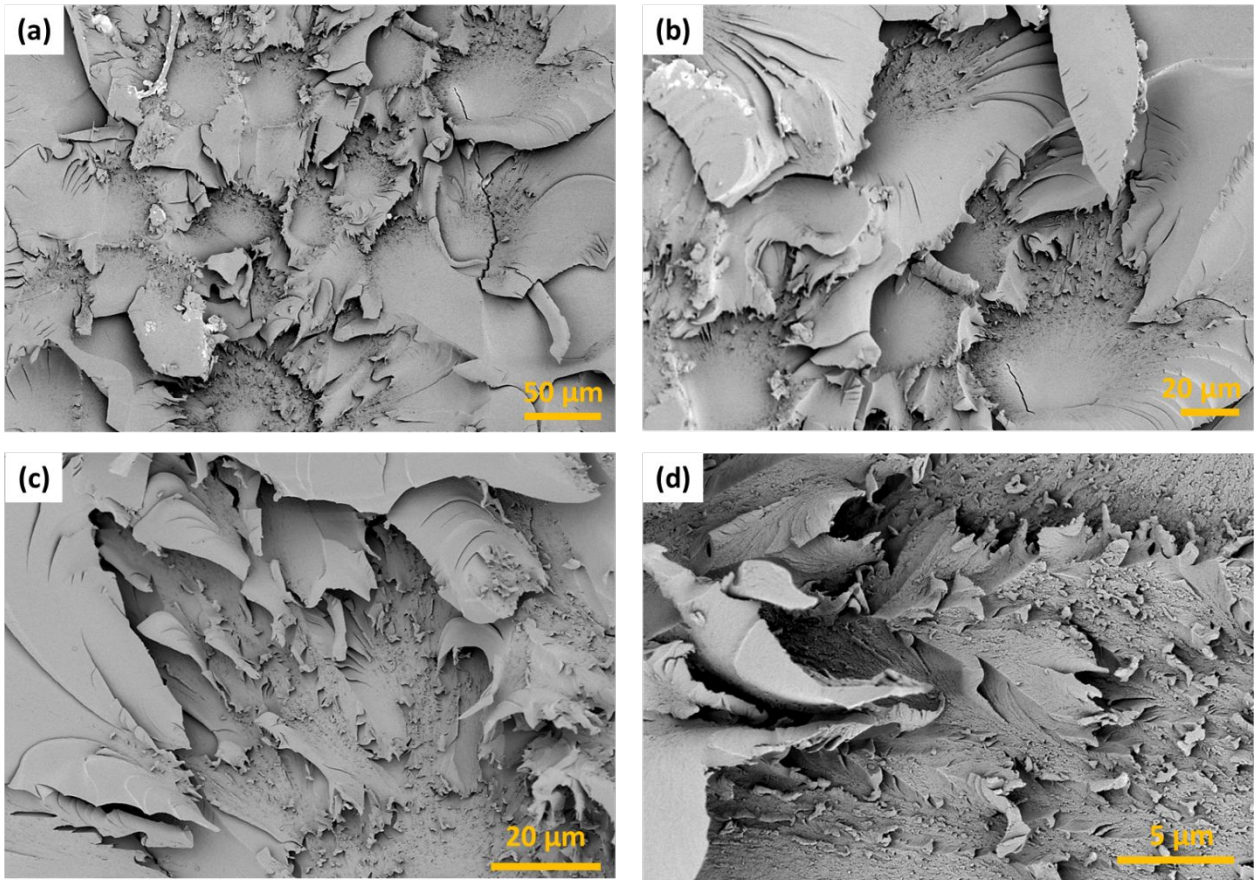

Figure S5: (a-d) SEM images of cured HSSM BMI fracture surface in the crack initiation and propagation region at different magnifications demonstrating intense plastic deformation.

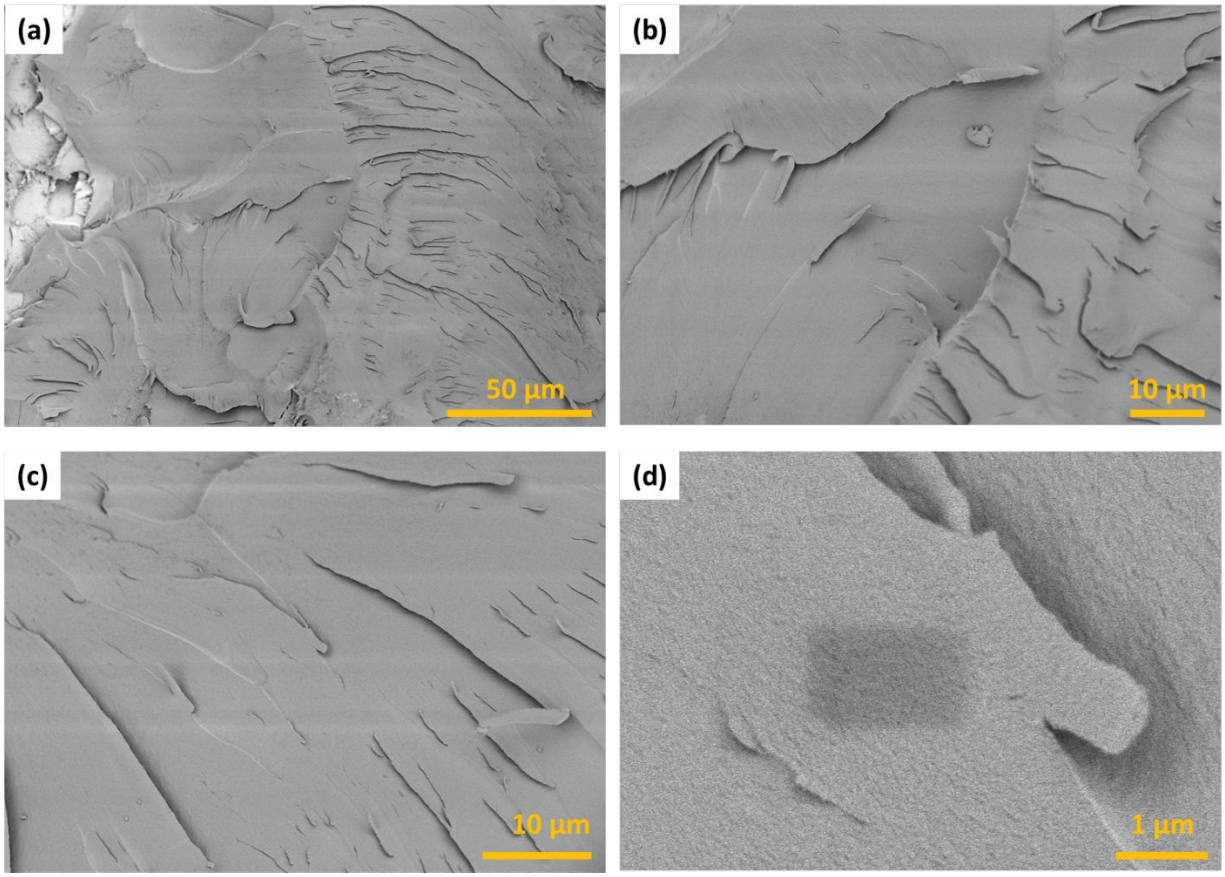

Figure S6: (a-d) SEM images of cured Melt BMI fracture surface in the crack initiation and propagation region at different magnifications. Much smoother fracture surface is observed compared to the HSSM BMI (Figure S5).

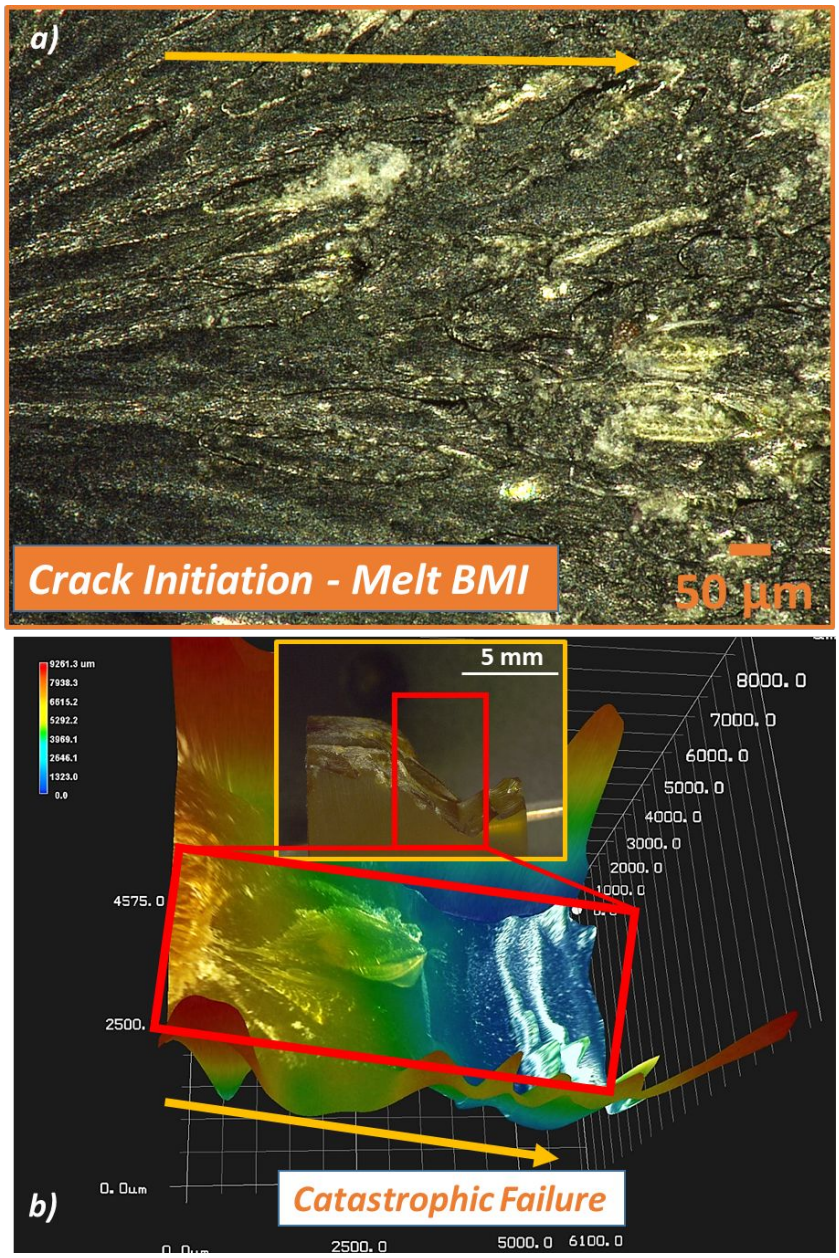

Figure S7 : (a) OM of the Melt BMI fracture surface in the crack initiation zone demonstrating streaks signifying crack propagation. No nodules are observed as were, for HSSM BMI. Yellow arrow points to the crack propagation direction. Yellow arrow points to the crack propagation direction. (b) 3D OM image of the Melt BMI demonstrating catastrophic failure.

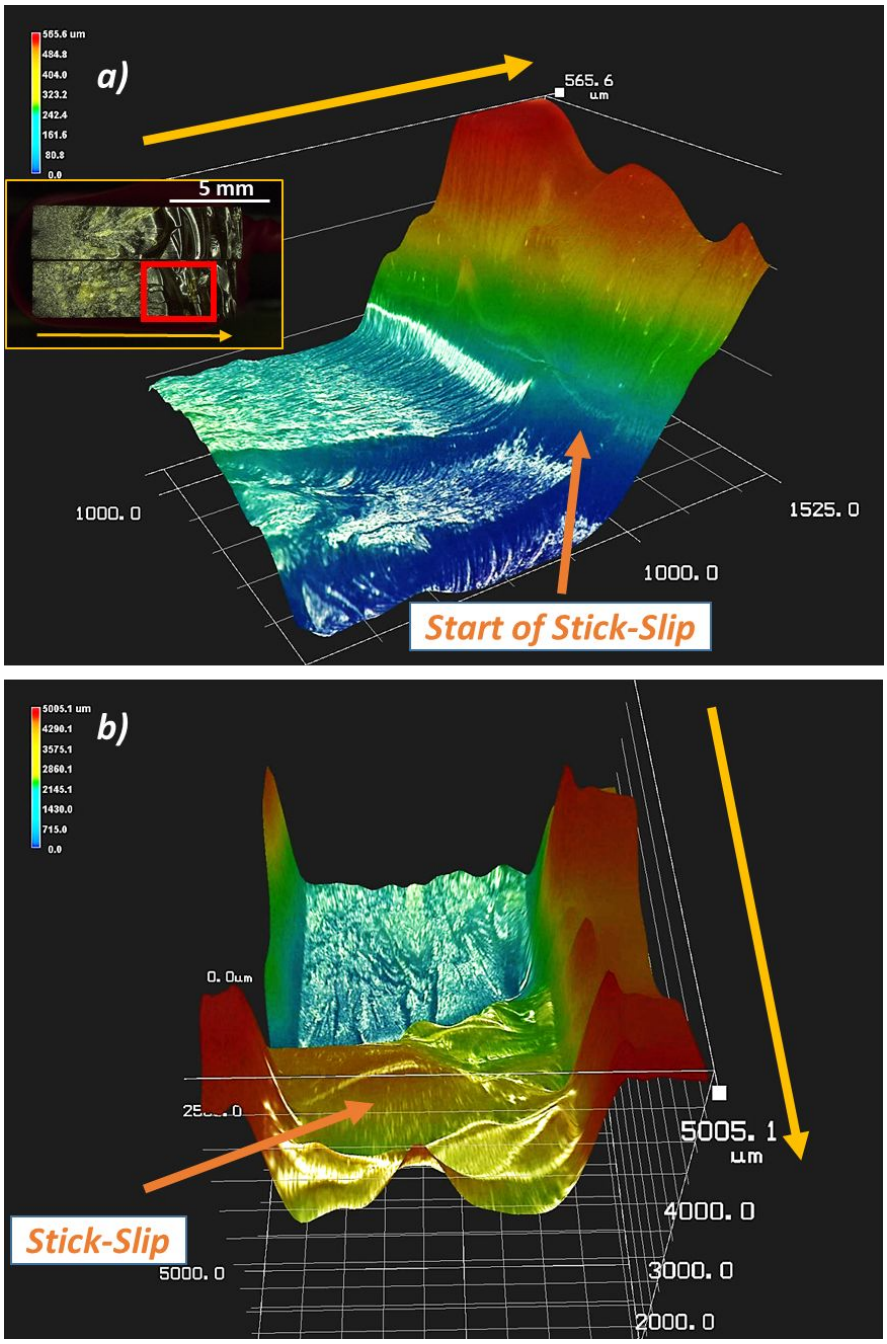

Figure S8 : (a and b) OM of HSSM BMI fracture surface at the transition zone from fast crack propagation to the stick-slip zone. Yellow arrow points to the crack propagation direction.

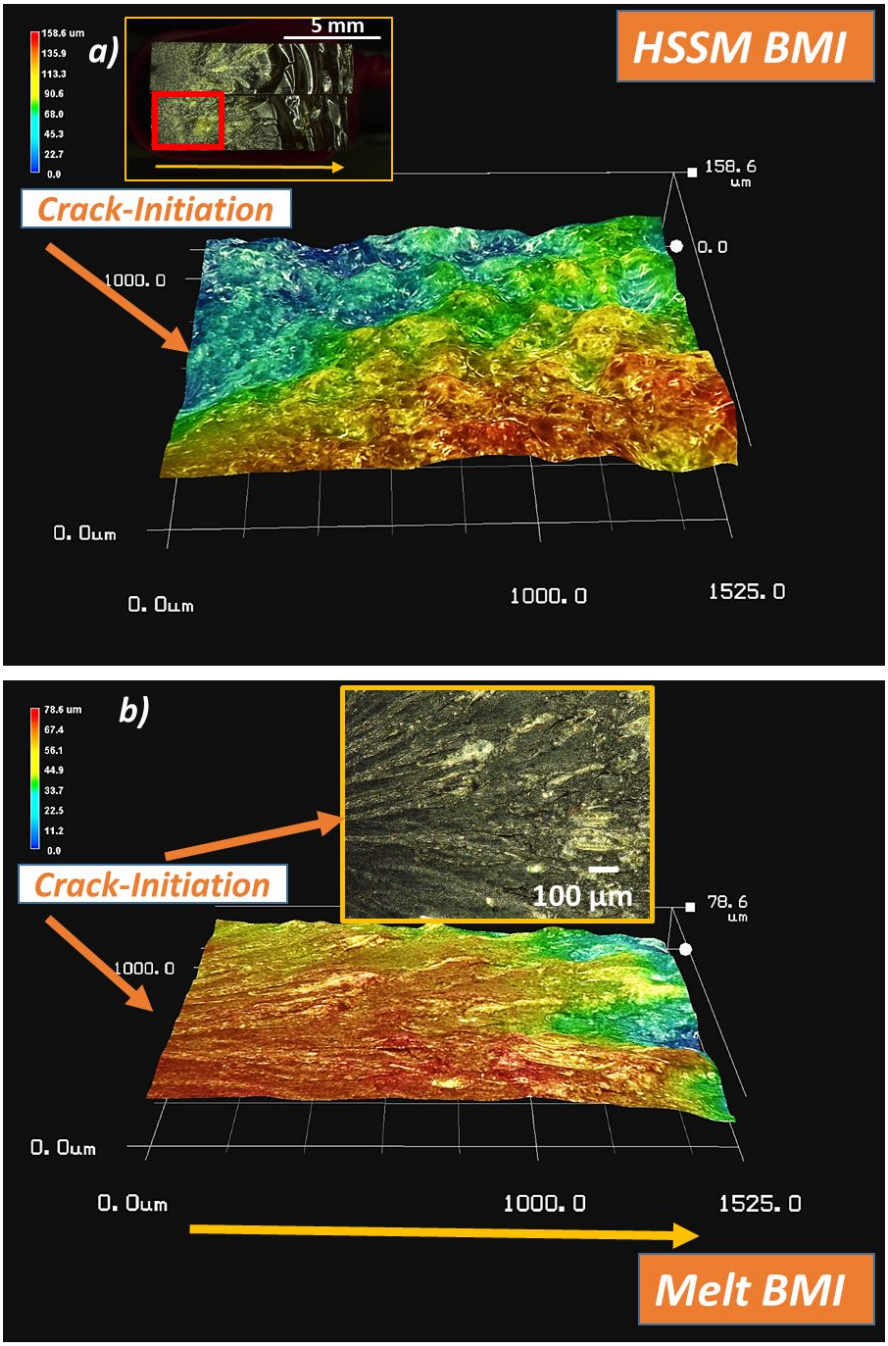

Figure S9 : OM of (a) HSSM BMI and (b) Melt BMI. HSSM BMI demonstrated about 2 times higher roughness in the crack initiation zone. Yellow arrow points to the crack propagation direction.

Abbreviations used in Table S1 and Table S2:

PEI – Polyethyleneimine

DOPO- 9,10-dihydro-9-oxa-10 phosphaphenanthrene-10-oxide

GO- Graphene oxide

RGO- Reduced graphene oxide

APTES- Aminopropyltriethoxysilane

MPTS- Methacryloxypropyl- trimethoxysilane

MAH- Maleic anhydride

HBPT- Hyperbranched polytriazine

OREC- Organic Rectorite

CE- Cyanate esters

MMt- Montmorillonite

Bz-Allyl - Bis allyl benzoxine

BADCy- Bisphenol A cyanate esters

IPN- Interpenetrating network

Table S1. Impact strength of p-BMI and BMI nanocomposites from literature.

Filler type	Filler loading (wt.%)	Impact Strength (kJ/m^2)	Mixing Method for BDM-DABA	Notes
p-CNT	0, 1	6.8, 7.8	Melt and add	Hyperbranched PEI f-CNTs, 2 component BMI, Izod impact test- ASTM D256.[7]
f-CNT	2.5	9.1		
p-CNT	0, 0.28	11.1, 7.8	Stirring	Amine f-CNTs, 2 component BMI, Unnotched izod impact test - ASTM 4812.[8]
f-CNT	0.28	15.3		
p-CNT	0, 1.5	4.7, -	Stirring	N-phenyl maleimide f-CNTs, 2 component BMI, Unnotched izod impact test - ASTM 4812. [9]
f-CNT	1.5	16		
p-CNT	0, 0.5	18, 24	Stirring	Diaminodiphenylmethane-f-CNTs, 2 component BMI, Charpy impact test post polishing with sand paper – ISO 179-2 [10]
f-CNT	0.5	30		
p-CNT	0, 0.75	9.8, 12.7	Stirring	Hyperbranched aliphatic polyimide f-CNTs, 2 component BMI, Izod impact test – ASTM D256. [11]
f-CNT	0.75	21.5		
p-CNT	0, 0.75	12.2, 16.6	Melt and add	p-CNTs, 2 component BMI [12]
DOPO; p-CNT	0; 0 4; 1	10.5 8.4	Stirring	DOPO used as flame retardant agent, Silane f-CNT, 2 component BMI, unnotched impact test- GB/T2571-1995.[13]
DOPO; f-CNT	4; 1	13		
GO	0, 0.3	12.5, 8	Melt and add	Silane f-GO by grafting MPTS on GO sheets, 2 component BMI, Unnotched impact test - ASTM 4812 using charpy impact testing machine.[14]
f-GO	0.3	20.8		
f-GO	0, 0.1	12.5, 23	Melt and add	APTES f-GO, 2 component BMI, Unnotched Impact Test - ASTM 4812 using charpy impact testing machine.[15]
f-GO	0, 0.1	12.5, 22	Melt and add	MAH f-GO, 2 component BMI, Unnotched Impact Test - ASTM 4812 using charpy impact testing machine. [16]
RGO	0, 0.6	10.7, 9.8	Stirring	HBPT f-RGO, 2 component BMI, GB/T2567-2008 standard for impact testing. [17]
f-RGO	0.6	16.7		
RGO	0, 0.3	18.8, 18	Stirring	Diazonium f-RGO, 2 component BMI, Unnotched Impact Test - ASTM 4812 using charpy impact testing machine.[18]
f-RGO	0.3	26.2		
OREC	0, 2	8.5, 11	Stirring	2 component BMI, GB 2517-95 Standard for impact testing.[19]

Table S2. Impact Strength of p-BMI and blends of BMI and their IPNs with thermosets and thermoplastics and their ternary nanocomposites from literature.

BMI blends/IPNs with thermosets and their ternary nanocomposites					
Resin/s; Filler	**BMI; Resin/s; (wt. %)**	**Filler (wt.%)**	**Impact Strength (kJ/m^2)**	**Mixing Method for BMI-Resin/s**	**Notes**
Bz-Allyl	100; 0	-	6.1	Stirring	BMI monomer, BDM blended with Bz-allyl, GB/T2567-2008 standard for impact testing.[20]
	70; 30	-	11.8		
BADCy; Bz-Allyl	43; 57; 0	-	12	Stirring	BMI monomer, BDM blended with BADCy in 3:4 ratio which further is blended with Bz-Allyl. GB/T2567-2008 standard for impact testing.[21]
	39; 52; 9	-	18		
BADCy; TDE-85	33; 67; 0	-	9.8	Stirring	BMI monomer, BDM blended with BADCy in 1:2 ratio which further is blended with TDE-85 epoxy, Unnotched impact test- GB/T2571-1995 standard.[22]
	27; 53; 20	-	13.5		
CE	-	-	10.1	-	Pre-polymerized BMI/CE was acquired and used. GB/T3960-1983 standard for impact testing.[23]
CE; p-CNT	-	0.6	10.6		
CE; f-CNT	-	0.6	13.7		
CE; OMMt	-	0	8.2	Stirring	BMI monomer, BDM blended with CE the ratio of which isn't specified, GB/T2567-2008 Standard for impact testing.[24]
	-	4	17.2		
BMI blends/IPNs with thermoplastics					
Resin/s; Filler	**BMI; Resin/s; Filler (weight %)**	**Filler**	**Impact Strength (KJ/m^2)**	**Mixing Method for BMI-Resin/s**	**Notes**
MEMBI; AE; PEK-C	80; 20; 0; 0	-	6.3	-	Two component BMI system modified with MEMBI, AE and PEK-C, GB1043-79 standard for impact testing. [25]
	64; 16; 0; 20	-	17		
	48; 12; 20; 20	-	18.9		

Table S3. Impact Strength of p-BMI cast under different processing and casting conditions. Levels connected by same letter are statistically similar.

Condition	Number of samples tested	Impact Strength (kJ/m^2)	Std. Dev	Statistical Connection letter
Melt BMI				
A	10	20	7	a
B1	5	14	2	a
B2	5	14	6	a
HSSM BMI				
A	10	37	12	b
B1	15	56	15	c
B2	**10**	**69**	**13**	**d**

The cure and post cure temperature and their duration were identical for all conditions, 4-hours at 191°C and 2-hours at 227°C, respectively. 3 variations in specimen casting conditions were explored:

a) Condition 'A'- Specimens are in the mold (cure + post cure) for complete duration.

b) Condition 'B1'- Specimens are in the mold while curing but free standing for post cure, that is, specimens are demolded while in the oven at curing temperature up on completion of cure cycle of 4 hours for further free-standing post-cure.

c) Condition 'B2'- Specimens are in the mold while curing but free standing for post cure, oven is cooled down to room temperature after completion of cure cycle, specimens are demolded, and oven is heated to post cure temperatures for free-standing post-cure.

Table S4. P-values illustrating the statistical significance of Impact strength data table S3. P-value smaller than 0.05 is considered statistically significant.

Processing type and cure condition	Melt "B1"	Melt "B2"	HSSM "A"	HSSM "B1"	HSSM "B2"
Melt "A"	0.3	0.3	0.003	<0.0001	<0.0001
Melt "B1"	X	0.9	0.001	<0.0001	<0.0001
Melt "B2"		X	0.002	<0.0001	<0.0001
HSSM "A"			X	0.0009	<0.0001
HSSM "B1"				X	0.014
HSSM "B2"					X

Table S5 : List of major FTIR and Raman peaks and their assignments.[1,26–28] The check mark represents a distinct observation of the corresponding peaks in this study in specimens including uncured and cured- Melt and HSSM BMI.

Wavenumber (cm^{-1})	Functional Group	FTIR	Raman
687	C=C—H (out-of-plane bending)	✓	
823	C=C (deformation mode)	✓	
787	C=O (Out of plane)		
947	C—C (maleimide)		
≈1110	C—O (Phenol/Ether)	✓	✓
1145	C—N—C (succinimide)	✓	
≈1169	C—N—C (maleimide)	✓	✓
≈1260	C—O (Phenol/Ester)	✓	✓
≈1395-1373	O=C—N (Ring)	✓	✓
1509	C=C (Aromatic)	✓	✓
1583	C=C Maleimide		✓
≈1605	C=C (Aromatic)		✓
1645	**Unassigned**		✓
1703	C=O (Carbonyl- asymmetric)	✓	
≈1776	C=O (Carbonyl- symmetric)		✓
≈2848	CH_2 (symmetric stretch)	✓	
≈2870	CH_3 (symmetric stretch)	✓	
≈2920	CH_2 (asymmetric stretch)	✓	
≈2960-2980	CH_3 (asymmetric stretch)	✓	

Table S6 : Activation energy and reaction kinetics parameters at various temperatures following Kissinger and Ozawa methods for Melt BMI and HSSM BMI

Kissinger method							
	E_a (kJ/mol)	A (s^{-1})	$k_{150\,°C}$	$k_{175\,°C}$	$k_{200\,°C}$	$k_{225\,°C}$	$k_{250\,°C}$
Melt	73	5×10^6	0.005	0.017	0.05	0.12	0.28
HSSM	83	57×10^6	0.003	0.012	0.04	0.11	0.28
Ozawa method							
	E_a (kJ/mol)	A (s^{-1})	$k_{150\,°C}$	$k_{175\,°C}$	$k_{200\,°C}$	$k_{225\,°C}$	$k_{250\,°C}$
Melt	75	8×10^6	0.005	0.016	0.05	0.12	0.28
HSSM	85	80×10^6	0.003	0.011	0.04	0.11	0.29

E_a- Cure activation energy
A - Pre-exponential factor
k – reaction rate constant at various temperatures

Table S7: Melt BMI and HSSM BMI exhibit statistically similar tensile properties. However, the properties are lower compared to the manufacturer reported values.[29]

	Tensile Strength (MPa)	**Tensile Modulus (GPa)**	**Strain at break (%)**
Melt	47 ± 7	3.6 ± 0.1	1.2 ± 0.2
HSSM	46 ± 15	3.6 ± 0.2	1.3 ± 0.5
Manufacturer reported	103	4.6	4.8

Table S8 : Tensile Strength of p-BMI cast under different processing and casting conditions. Levels connected by same letter are statistically similar

Condition	**Number of samples tested**	**Tensile Strength (MPa)**	**Std. Dev**	**Statistical Connection letter**
Melt BMI				
A	10	51	16	a
B1	5	57	13	a
B2	5	47	7	a
HSSM BMI				
A	10	53	14	a
B1	15	50	12	a
B2	10	46	15	a

Table S9 : P-values showing the statistical significance of tensile strength data in table S5. P-value smaller than 0.05 is considered statistically significant.

Processing type and cure condition	Melt "B1"	Melt "B2"	HSSM "A"	HSSM "B1"	HSSM "B2"
Melt "A"	0.55	0.62	0.78	0.89	0.46
Melt "B1"	X	0.34	0.7	0.46	0.23
Melt "B2"		X	0.47	0.67	0.9
HSSM "A"			X	0.65	0.3
HSSM "B1"				X	0.49
HSSM "B2"					X

Table S10 *:* Tensile Modulus of p-BMI cast under different processing and casting conditions. Levels connected by same letter are statistically similar.

Condition	**Number of samples tested**	**Tensile Modulus (GPa)**	**Std. Dev**	**Statistical Connection letter**
Melt BMI				
A	10	4	0.3	a, b
B1	5	3	0.3	e
B2	5	3.6	0.1	b, c, d
HSSM BMI				
A	10	3.6	0.4	b, c
B1	15	4.1	0.4	a
B2	10	3.6	0.2	c

Table S11 : P-values showing the statistical significance of tensile modulus data in table S7. P-value smaller than 0.05 is considered statistically significant.

Processing type and cure condition	Melt "B1"	Melt "B2"	HSSM "A"	HSSM "B1"	HSSM "B2"
Melt "A"	<0.0001	0.11	0.058	0.42	0.039
Melt "B1"	X	0.01	0.0022	<0.0001	0.0044
Melt "B2"		X	0.93	0.022	0.91
HSSM "A"			X	0.0046	0.8
HSSM "B1"				X	0.003
HSSM "B2"					X

Table S12 *:* Strain at break of p-BMI cast under different processing and casting conditions. Levels connected by same letter are statistically similar.

Condition	**Number of samples tested**	**Strain at break (%)**	**Std. Dev**	**Statistical Connection letter**
Melt BMI				
A	10	1.3	0.5	a
B1	5	2.2	0.5	b
B2	5	1.2	0.2	a
HSSM BMI				
A	10	1.6	0.3	a
B1	15	1.1	0.3	a
B2	10	1.3	0.5	a

Table S13 : P-values showing the statistical significance of strain to break data in table S9. P-value smaller than 0.05 is considered statistically significant.

Processing type and cure condition	Melt "B1"	Melt "B2"	HSSM "A"	HSSM "B1"	HSSM "B2"
Melt "A"	0.0015	0.84	0.24	0.48	0.86
Melt "B1"	X	0.0032	0.02	0.0003	0.001
Melt "B2"		X	0.25	0.7	0.95
HSSM "A"			X	0.07	0.19
HSSM "B1"				X	0.59
HSSM "B2"					X

References

(1) Phelan, J. C.; Sung, C. S. P. Cure Characterization in Bis(Maleimide)/Diallylbisphenol A Resin by Fluorescence, FT-IR, and UV-Reflection Spectroscopy. *Macromolecules* **1997**, *30* (22), 6845–6851.

(2) Curliss, D. B.; Cowans, B. A.; Caruthers, J. M. Cure Reaction Pathways of Bismaleimide Polymers: A Solid-State 15N NMR Investigation. *Macromolecules* **1998**, *31* (20), 6776–6782.

(3) Mijović, J.; Andjelić, S. Study of the Mechanism and Rate of Bismaleimide Cure by Remote In-Situ Real Time Fiber Optic Near-Infrared Spectroscopy. *Macromolecules* **1996**, *29* (1), 239–246.

(4) Iredale, R. J.; Ward, C.; Hamerton, I. Modern Advances in Bismaleimide Resin Technology: A 21st Century Perspective on the Chemistry of Addition Polyimides. *Prog. Polym. Sci.* **2017**, *69*, 1–21.

(5) Pritchard, G.; Swan, M. THE CROSSLINKING OF EUTECTIC MIXTURES OF BISMALEIMIDES. *Fur. Polym. J* **1993**, *29* (23), 357–363.

(6) Deng, S.; Hou, M.; Ye, L. Temperature-Dependent Elastic Moduli of Epoxies Measured by DMA and Their Correlations to Mechanical Testing Data. *Polym. Test.* **2007**, *26* (6), 803–813.

(7) Qiu, J.; Wu, qianqian; Jin, lei. Effect of Hyperbranched Polyethyleneimine Grafting Functionalization of Carbon Nanotubes on Mechanical, Thermal Stability and Electrical Properties of Carbon Nanotubes/Bismaleimide Composites. *RSC Adv.* **2016**, *6*, 96245–96249.

(8) Gu, A.; Liang, G.; Liang, D.; Ni, M. Bismaleimide/Carbon Nanotube Hybrids for Potential Aerospace Application: I. Static and Dynamic Mechanical Properties. *Polym. Adv. Technol.* **2007**, *18* (10), 835–840.

(9) Wang, C.; Liu, L. N-Phenyl Maleimide Grafted MWNT/Bismaleimide-Allyl Bisphenol A Nanocomposites: Improved MWNT Dispersion, Resin Reactivity and Composite Mechanical Strength. *Mater. Lett.* **2017**, *194*, 38–41.

(10) Han, Y.; Zhou, H.; Ge, K.; Guo, Y.; Liu, F.; Zhao, T. Toughness Reinforcement of Bismaleimide Resin Using Functionalized Carbon Nanotubes. *High Perform. Polym.* **2014**, *26* (8), 874–883.

(11) Xiong, L.; Qin, X.; Liang, H.; Huang, S.; Lian, Z. Preparation and Properties of Nanocomposites Based on Hyperbranched Aliphatic Polyamide Functionalized Multiwalled Carbon Nanotubes and Bismaleimide Resin. *Polym. - Plast. Technol. Eng.* **2014**, *53* (15), 1607–1614.

(12) Li, S.; Zhao, X. Y.; Wang, X. Preparation and Properties of CNTs Reinforced BMI/DBA Nanocomposites. *Adv. Mater. Res.* **2015**, *1120–1121*, 357–360.

(13) Wang, Z.; Wu, W.; Zhang, X.; Wang, J.; Liu, B. Effects of Silane-Modified Multiwalled Carbon Nanotubes and 9,10-Dihydro-9-Oxa-10 Phosphaphenanthrene-10-Oxide on the Flame Retardancy and Mechanical Properties of Bismaleimide Resin. *High Perform. Polym.* **2016**, *28* (7), 831–841.

(14) Li Wei A4 - Zhou, Baoquan A4 - Wang, Mingyu A4 - Li, Zhonghui A4 - Ren, Rong, W. A.-L. Silane Functionalization of Graphene Oxide and Its Use as a Reinforcement in Bismaleimide Composites. *J. Mater. Sci.* **2015**, *v. 50* (16), 5402-5410–2015 v.50 no.16.

(15) Li, W.; Xue, F.; Li, Q. Modification of Bismaleimide Resin by Using γ-Aminopropyl Triethoxysilane Functionalised Graphene Oxide. *Plast. Rubber Compos.* **2018**, *47* (5), 187–191.

(16) Li, W.; Wang, M.; Yue, Y.; Ji, W.; Ren, R. Enhanced Mechanical and Thermal Properties of Bismaleimide Composites with Covalent Functionalized Graphene Oxide. *RSC Adv.* **2016**, *6* (59), 54410–54417.

(17) Liu, C.; Yan, H.; Chen, Z.; Yuan, L.; Lv, Q. Effect of Surface-Functionalized Reduced Graphene Oxide on Mechanical and Tribological Properties of Bismaleimide Composites. *RSC Adv.* **2015**, *5* (58), 46632–46639.

(18) Liu, M.; Duan, Y.; Wang, Y.; Zhao, Y. Diazonium Functionalization of Graphene Nanosheets and Impact Response of Aniline Modified Graphene/Bismaleimide Nanocomposites. *Mater. Des.* **2014**, *53*, 466–474.

(19) Yuan, L.; Ma, X.; Gu, A.; Yan, H.; Liang, G.; Wang, W.; Wu, J. A Novel Organic Rectorite Modified Bismaleimide/Diallylbisphenol A System. *Polym. Adv. Technol.* **2009**, *20* (11), 826–833.

(20) Wang, Y.; Kou, K.; Zhuo, L.; Chen, H.; Zhang, Y.; Wu, G. Thermal, Mechanical and Dielectric Properties of BMI Modified by the Bis Allyl Benzoxazine. *J. Polym. Res.* **2015**, *22* (4), 51.

(21) Wang, Y.; Kou, K.; Wu, G.; Feng, A.; Zhuo, L. The Effect of Bis Allyl Benzoxazine on the Thermal, Mechanical and Dielectric Properties of Bismaleimide–Cyanate Blend Polymers. *RSC Adv.* **2015**, *5* (72), 58821–58831.

(22) Wu, G.; Kou, K.; Chao, M.; Zhuo, L.; Zhang, J.; Li, N. Preparation and Characterization of Bismaleimide-Triazine/Epoxy Interpenetrating Polymer Networks. *Thermochim. Acta* **2012**, *537*, 44–50.

(23) Li, P.; Li, T.; Yan, H. Mechanical, Tribological and Heat Resistant Properties of Fluorinated Multi-Walled Carbon Nanotube/Bismaleimide/Cyanate Resin Nanocomposites. *J. Mater. Sci. Technol.* **2017**, *33* (10), 1182–1186.

(24) Wu, G.; Cheng, Y.; Wang, K.; Wang, Y.; Feng, A. Fabrication and Characterization of OMMt/BMI/CE Composites with Low Dielectric Properties and High Thermal Stability for Electronic Packaging. *J. Mater. Sci. Mater. Electron.* **2016**, *27* (6), 5592–5599.

(25) BAOYAN, Z.; PING, L. I.; XIANGBAO, C. Studies of Modified Bismaleimide Resins Part I The Influence of Resin Composition on Thermal and Impact Properties. *J. Mater. Sci.* **1998**, *33* (23), 5683–5687.

(26) Parker, S. F.; Mason, S. M.; Williams, K. P. J. *Fourier Transform Raman and Infrared Spectroscopy of N-Phenylmaleimide and Methylene Dianiline Bismaleimide*; 1990; Vol. 46.

(27) Xu, X.; Wang, X.; Liu, W.; Zhang, X.; Li, Z.; Du, S. Microwave Curing of Carbon Fiber/Bismaleimide Composite Laminates: Material Characterization and Hot Pressing Pretreatment. *Mater. Des.* **2016**, *97*, 316–323.

(28) Sava, M.; Gaina, C.; Gaina, V.; Timpu, D. Synthesis and Characterization of Some Bismaleimides Containing Ether Groups in the Backbone. *Macromol. Chem. Phys* **2001**, *202*, 2601–2605.

(29) CYCOM 5250-4 RTM | Solvay https://www.solvay.com/en/product/cycom-5250-4-rtm (accessed Jul 12, 2019).